

Paweł LAJMERT¹

AN APPLICATION OF HILBERT-HUANG TRANSFORM AND PRINCIPAL COMPONENT ANALYSIS FOR DIAGNOSTICS OF CYLINDRICAL PLUNGE GRINDING PROCESS

This paper presents a sensor based diagnostic system for a cylindrical plunge grinding process which ensures a reliable process state and tool wear identification. A new signal processing technique, i.e. Hilbert-Huang transform (HHT) was evaluated for this purpose based on the vibration and acoustic emission signal measurements. Numerical and experimental studies have demonstrated that the process state and tool wear may be effectively detected through a statistical analysis of the time-dependent amplitudes and instantaneous frequencies resulting from the HHT. A principal component analysis was used to diagnose different grinding process states.

1. INTORODUCTON

Automatic supervision of cylindrical grinding processes is still a challenge. The objective of the grinding process supervision is to diagnose incipient and abrupt symptoms of undesired process states or tool wear so that adequate continuous or gradual adjustments of basic kinematic parameters could be carried out to maintain the process in the optimal working region [1,2]. An essential prerequisite of satisfying these requirements is the use of effective signal processing techniques to find features in measured signals strongly correlated with undesired process states and tool wear. From a variety of monitoring techniques the vibration and acoustic emission measurements seems to be the most realistic approaches [1,3]. When using appropriate signal decomposition techniques the features hidden in these signals can be extracted and an estimation of the grinding results can be done. Unfortunately, the measured signals are in most cases nonlinear and nonstationary in nature. These signals originate from different sources, such as friction, grain impacts, plastic deformations, grain and bond fracture, grinding burn and also from the grinding chatter phenomenon [3]. These sources of information emit interfering waves, which makes the process of its separation very difficult. Consequently, due to the transient and nonstationary

¹ Technical University of Łódź, Institute of Machine Tools and Production Engineering, Poland

nature of the analyzed signals the currently used traditional methods based on Fourier transform, which assume signal stationarity, are inappropriate for the monitoring of grinding processes.

Recently, time-frequency analysis techniques, mainly short-time Fourier transform (STFT) and wavelet transform (WT) have been widely investigated for the monitoring of machining processes [4]. However, these methods were designed only for analysis of linear signals and moreover they require the choice of many preliminary parameters. In the case of STFT a selection of the appropriate size of the processing window is required to correspond with the frequency of the signal analyzed. Whereas, using the wavelet transform the results rely to a great extent on the parent wavelet employed, basic wavelet function and the discretization of scales [5,7,8]. Improper selection of any of these numerous parameters may significantly reduce the applicability of these methods in analyzing nonstationary and nonlinear signals. For these reasons a strong need for a new signal processing technique is well visible. This paper investigates the use of a newly developed technique, i.e. Hilbert-Huang transform, for the diagnostics of plunge grinding process based on vibration and raw acoustic emission signals.

2. DESCRIPTION OF HILBERT-HUANG TRANSFORM

The Hilbert-Huang transform uses two processing techniques, i.e. empirical mode decomposition (EMD) and Hilbert spectral analysis [5]. It is an adaptive method designed particularly for analyzing nonlinear and nonstationary data changing even within one oscillation cycle. The EMD decomposes time-series into a set of intrinsic mode functions (IMFs) which represent simple oscillatory modes, but unlike the simple harmonic functions they can have variable amplitude and frequency along the time. The EMD decomposes data in a few steps. First, it identifies all the local extrema of the signal, i.e. minima and maxima points. These extrema are next interpolated by cubic splines that form the upper and lower envelopes of the analyzed signal, see Fig. 1a.

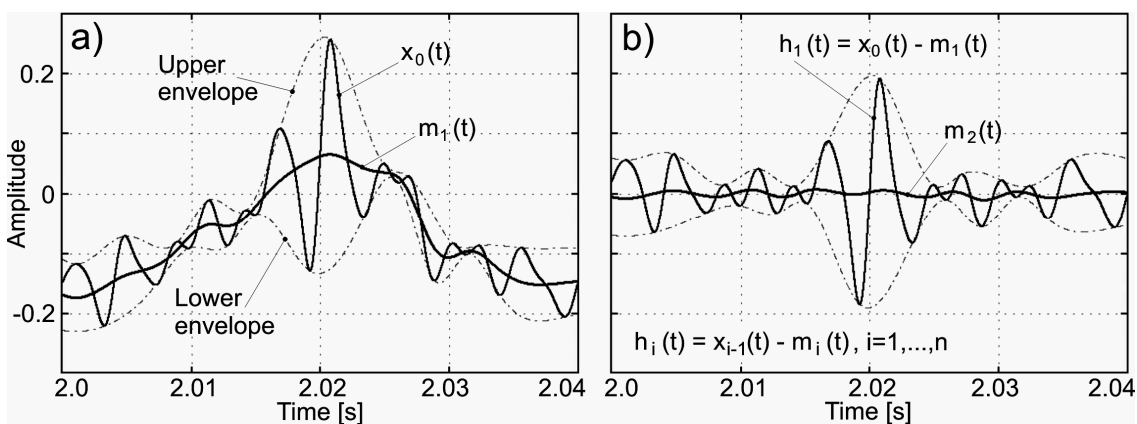


Fig. 1. Illustration of the sifting process: a) the original data with the upper, lower envelope and resultant mean line; b) the data after the first sifting process

Next, a mean line $m_1(t)$ between the upper and lower envelopes is computed and subtracted out from the original signal $x_0(t)$. As a result, new data $h_1(t)$ are obtained, see Fig. 1b. This procedure is called a sifting process and is repeated on the successive data $h_i(t)$ until at any point the mean line between the upper and lower envelopes is near zero, see Fig. 1b. At this point, the first IMF component is found $c_1(t)=h_n(t)$ which should represent the finest scale or the shortest period component of the signal $x_0(t)$. In the next step, this first IMF component $c_1(t)$ is extracted from the original data $x_0(t)$ and the whole sifting process is repeated on a new data $x_1(t)=x_0(t)-c_1(t)$ to obtain the successive components of increasing period with the last treated as a residue. The second part of HHT consists of Hilbert transform which is performed on each IMF component separately. Thus, it is possible to obtain the instantaneous frequencies and amplitudes of the signal analyzed. With Hilbert transform any signal $x(t)$ may be transformed into a complex function by adding a complex part $y(t)$ which actually is the same as $x(t)$ but shifted in phase by 90 degrees. Having such a representation of the signal the instantaneous amplitude $a(t)$ and frequency $\omega(t)$ functions may be given by the following formulas:

$$a(t) = \sqrt{x^2(t) + y^2(t)}, \quad \omega(t) = \frac{d}{dt} (\tan^{-1}(y(t)/x(t))) \tag{1,2}$$

To verify the usefulness of above described method a test signal was created composed of three pairs of interfering, exponentially changing sinusoidal waves of different frequencies and of different duration times to simulate long-lasting signals and burst signals which may be found in acoustic emission signal measurements, see Fig. 2a. The interfering waves were moved in phase by 2 radians. The results for HHT transform are shown in Fig. 2b. As may be seen the HHT gives very sharp time-frequency representation of the signal analyzed.

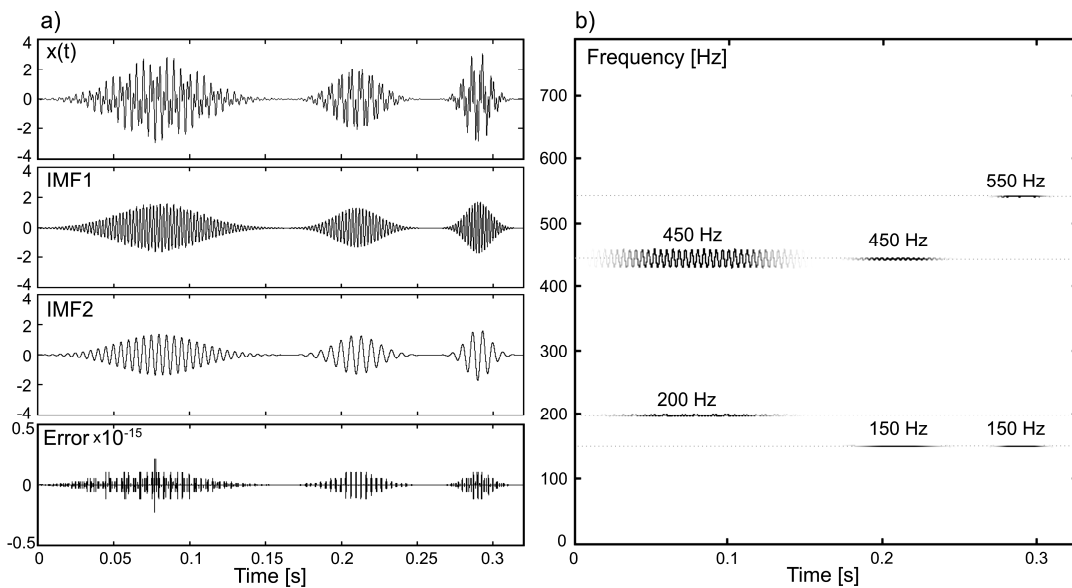


Fig. 2. Results for HHT transform: a) the test signal, IMF components and amplitude error; b) The Hilbert spectrum HHT(t,ω)

The results received using HHT were compared to these obtained by two traditional methods, i.e. STFT and continuous WT, see Fig. 3. As may be seen, the STFT and wavelet transform spreads the energy in the frequency and time domain. In the case of the wavelet transform the main problem is to select the best basic wavelet function. When improperly selected, the results may be even worse than these obtained by STFT method.

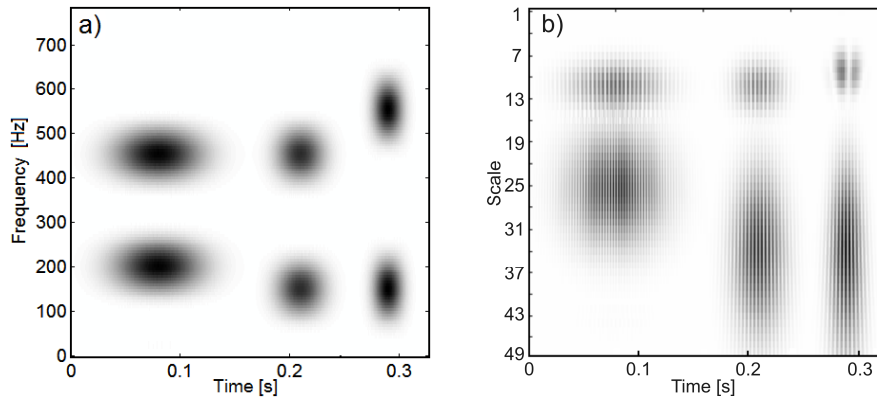


Fig. 3. Results of test signal analysis using: a) short-time Fourier transform; b) continuous wavelet transform for Morlet basic wavelet function

3. EXPERIMENTAL TESTS

In order to evaluate the usefulness of HHT method for the grinding process diagnostics several experimental investigations were carried out on a common cylindrical grinding machine equipped with adequate measurement units [6]. A vitrified 38A80KVBE grinding wheel was used. The workpieces were made of 34CrAl6C steel hardened to 50 HRC. The research was carried out at different working regions, connected with the grinding burn and increased grinding chatter growth. For this purpose the workpiece rotational speed was changed in a wide range from 0.7 to 2.0 rev/s. The grinding cycle was composed of a roughing phase and a rapid retraction of the grinding wheel. The infeed velocity of the grinding wheel v_{fr} was the same for all the tests, equal to about 12 $\mu\text{m/s}$, so as to keep the material removal rate at constant level. Tests were continued until the end of the wheel life. To characterize the process state, the grinding vibration and raw acoustic emission signals were measured using sensors attached to the tailstock centre. After each grinding test the workpiece waviness errors were measured with the use of a specially designed measurement device with a wide measurement range and supported with a diamond gauging tip adapted from a roughness measuring device.

4. ANALYSIS OF VIBRATION SIGNAL AND WORKPIECE WAVINESS ERRORS

First, the ability of HHT for analyzing chatter vibrations, i.e. separation of frequency modes and detection of its growth was investigated. Vibrations were measured with

a frequency 100 kHz. In Fig. 4a a HHT spectrum of exemplified vibration signal is shown. As may be seen, the energy of each IMF is spread in a wide frequency range, which indicates the nonlinear and nonstationary nature of the vibration signal. However, since the energy is represented in the form of separate IMF components, the course of IMFs may be averaged in the frequency domain, see Fig. 4a. Thanks to that the individual vibration modes may be clearly differentiated and its mean frequency estimated, which would be directly impossible when using other decomposition methods. Such an averaged IMFs characteristics of the vibration signal for the sharp and the worn grinding wheel are shown in Fig. 4b. They display a significant increase of the IMFs amplitudes for the worn grinding wheel.

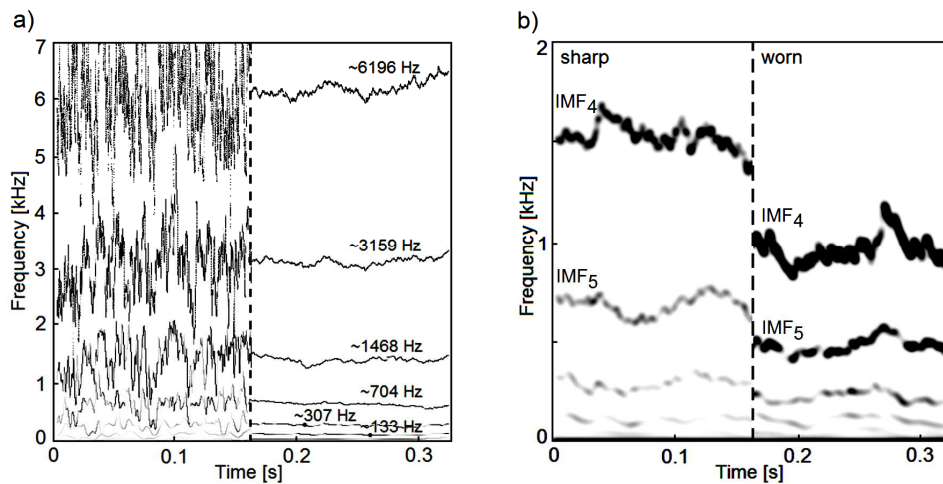


Fig. 4. The HHT spectrum: a) of exemplified vibration signal; b) of averaged IMFs for sharp and worn grinding wheel ($n_w=2.0$ rev/s)

Analysis of all the IMF components indicates that this increase may be especially observed for frequencies of about 740 Hz and 1400 Hz (fifth and fourth IMF). Moreover, the significant decrease of frequency level of these vibration modes for worn grinding wheel is well visible. This decrease may be caused by a change of stiffness and damping in the grinding contact area. To verify the physical meaning of these vibration modes a model of the workpiece and supporting system was created with the use of the finite element method. It turned out that the dominant vibration modes fit well to the first few transverse vibrations of the workpiece, see Fig. 5. Using the model the following frequencies of vibration modes were found: 138 Hz, 343 Hz, 753 Hz, 967 Hz, 1327 Hz. Apart from the fourth frequency (967 Hz), they correspond well with the frequencies shown in Fig. 5.

In Fig. 6 the amplitude increases of IMFs corresponding to the dominating vibration modes are shown for low and high workpiece rotational speeds. It may be seen that the influence of the workpiece peripheral speed on chatter development is almost insignificant.

The second part of the research was connected with the analysis of waviness errors of the workpiece. The most obvious results on the workpiece are the so-called chatter marks [3]. The HHT was used to quantify these waviness errors. In Fig. 7 the mean amplitudes of dominant IMF components of waviness errors are shown. After an analysis it turned out that

the frequency of IMF waviness components multiplied by the workpiece rotational speed quite well correspond to the dominant vibration modes of the shaft. Thanks to this a mapping of vibration IMFs on waviness errors seems to be possible.

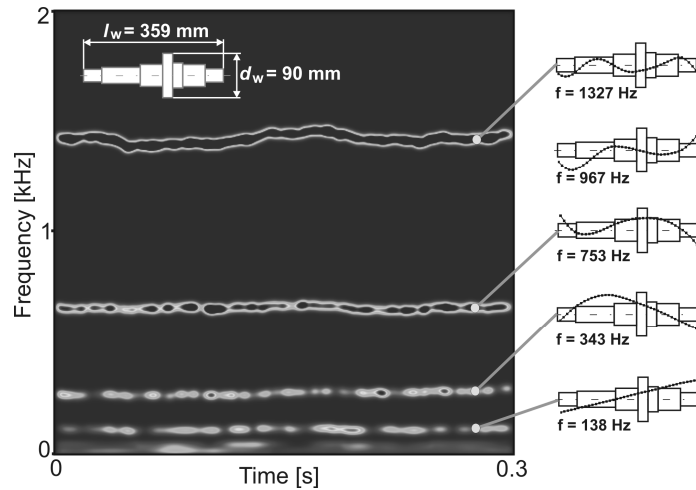


Fig. 5. The HHT spectrum of a vibration signal and corresponding vibration modes of the shaft being ground

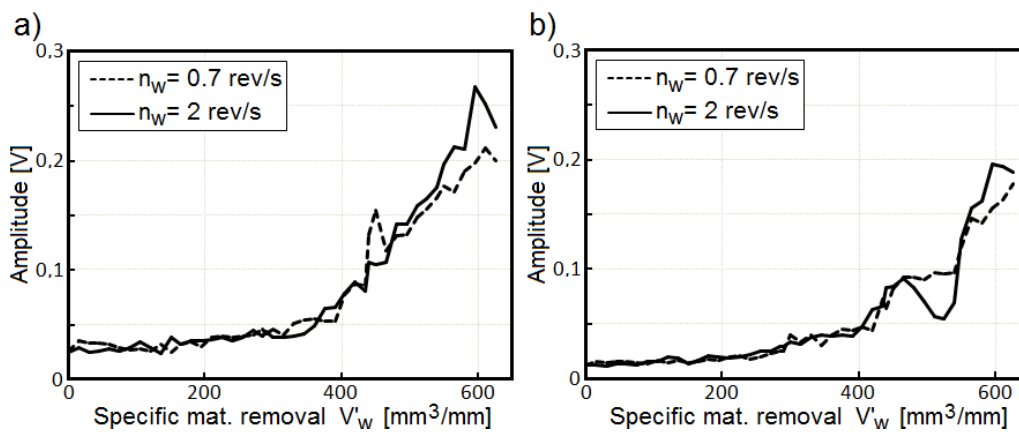


Fig. 6. Changes of mean amplitude of IMF components during grinding: a) fourth IMF; b) fifth IMF

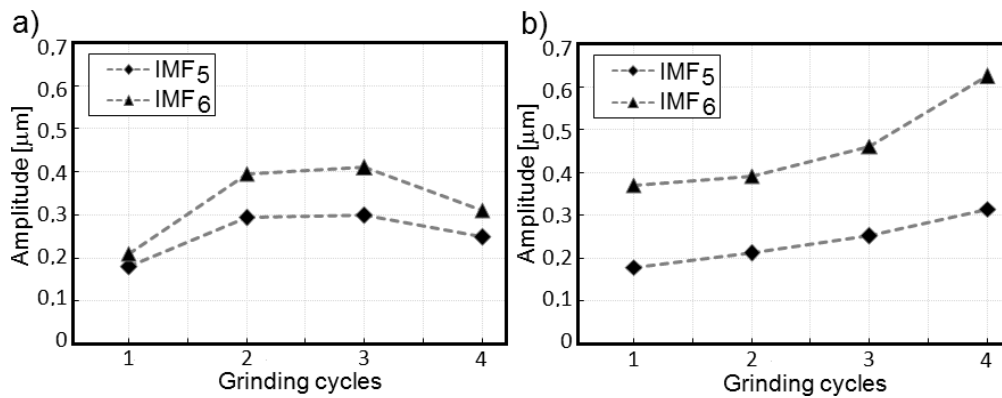


Fig. 7. Changes of amplitude of the fifth and sixth IMF component of workpiece waviness errors for the successive grinding cycles: a) workpiece rotational speed $n_w = 0.7$ rev/s; b) $n_w = 2$ rev/s

5. ANALYSIS OF ACOUSTIC EMISSION SIGNAL

In Fig. 8 an exemplified HHT spectrum of AE signal is presented. After an analysis, it can be found that this spectrum shows a special activity for a few, well distinguished frequencies equal to about $f_{IMF1}=240$, $f_{IMF2}=115$, $f_{IMF3}=55$ and $f_{IMF4}=24$ kHz.

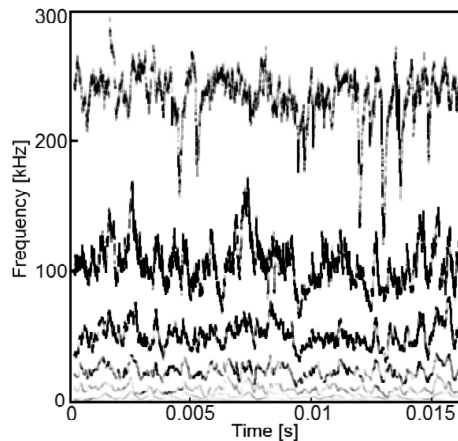


Fig. 8. An exemplified HHT spectrum of AE signal

The first IMF component of the highest frequency corresponds to the phenomena of acoustic emission generation, such as grain and bond fracture, e.g. during the grinding wheel self-sharpening or during the grinding burn. The variation of this IMF component for sharp and worn grinding wheel as well as for high and low workpiece peripheral speed is shown in Fig. 9. As may be seen for low workpiece peripheral speed a sudden changes of IMF amplitude appear which are the symptom of grinding burn, see Fig. 9b. The IMF components of lower frequencies relate to basic deformation mechanisms, undergoing in the workpiece material.

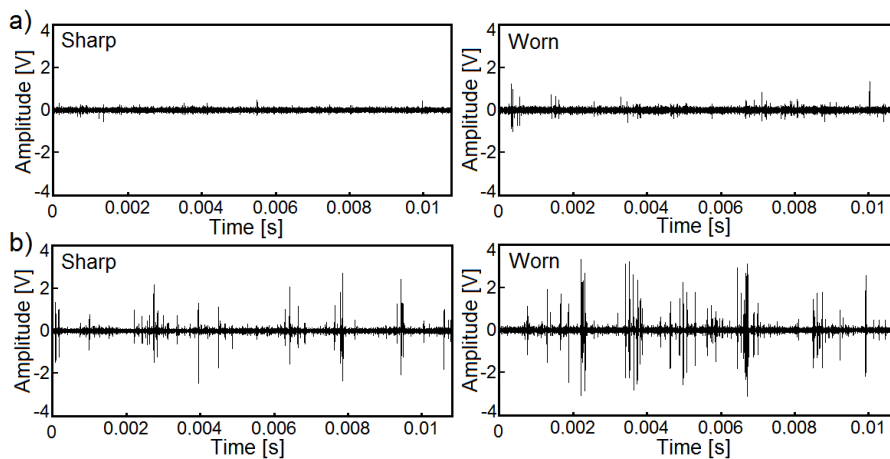


Fig. 9. The course of the first AE IMF component for sharp and worn grinding wheel: a) high workpiece rotational speed $n_w=2$ rev/s, b) low workpiece rotational speed $n_w=0.7$ rev/s

The AE IMFs reveal other important features. For instance, a mean frequency, especially for the second IMF component, decreases significantly with the tool wear, whereas a mean amplitude increases, see Fig. 10. This may be connected with the decreasing number of the grinding wheel active abrasive grains.

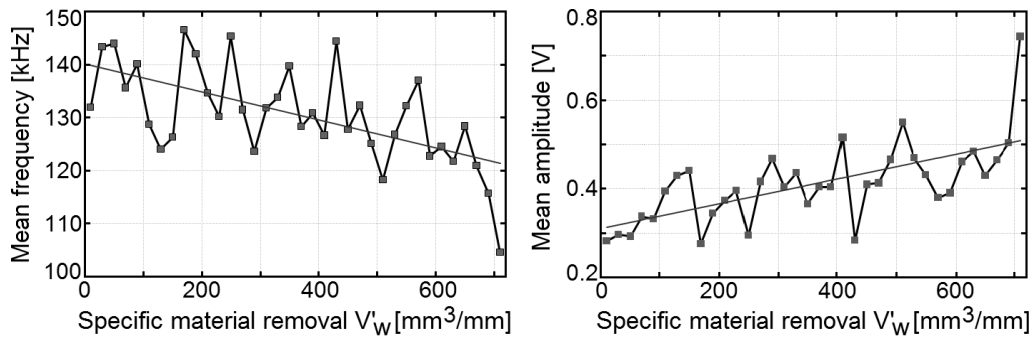


Fig. 10. The variation of mean frequency and mean amplitude (with a trend line) of the second AE IMF component ($f_{IMF2} = 115\text{kHz}$), $n_w = 0.7\text{ rev/s}$

6. DESCRIPTION OF THE DIAGNOSTIC SYSTEM

A structure of the diagnostic system applying HHT is shown in Fig. 11. Basically, this approach employs HHT transform for the separation of transient and continuous components of the signals measured, feature extraction procedure and principal component analysis (PCA) for the process state and tool wear classification. The PCA was also used to reduce the dimensionality of feature patterns without a significant loss of information.

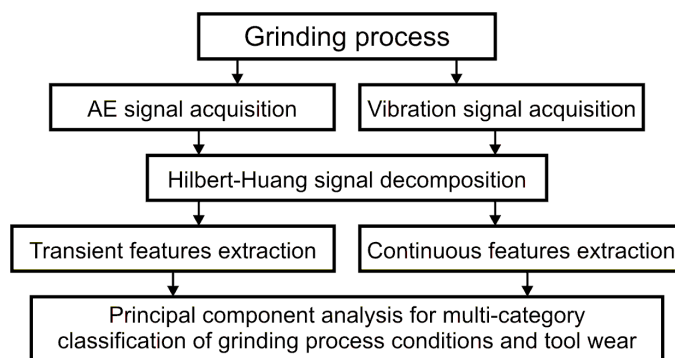


Fig. 11. General structure of the diagnostic system

In order to compute a principal component matrixes for the vibration and AE data a set of features was created for different grinding conditions involving states for sharp and worn grinding wheel as well as for low and high workpiece peripheral speeds. The feature vector was composed of maximum, mean value, standard deviation, kurtosis and skew of real

value, instantaneous amplitude and frequency of selected vibration and AE IMF components. After a preliminary analysis the fourth and fifth components were chosen for the vibration signal (see Fig. 4b) while for the AE signal the first and the second (see Fig. 8a). Due to the large size of the feature vector (15 features for each IMF component) a principal component analysis was carried out to reduce the dimensionality of data without any significant loss of information. As a result, the feature vector was reduced by more than 83% for the vibration data, while for the AE data by 40%. The selected features and its average weight are shown in Table 1.

Table 1. Selected features and its relative importance

	Max. value	Mean value	Standard deviation	Kurtosis	Skew
Real IMF			■ □	□	
IMF amplitude	■ □	■ □	■ □	□	□
IMF frequency		■ □	■ □		
■ - Vibration signal □ - Acoustic emission signal					

In Table 2 the changes of the most significant features for the vibration signal are presented. As may be seen, these features are strongly correlated with the tool wear.

Table 2. Changes of the most significant features for vibration signal ($n_w=2\text{rev/s}$)

IMF no	Grinding wheel condition	Mean Ampl. [V]	Mean Freq. [Hz]	Max. Ampl. [V]	Std. Dev. IMF	Std. Dev. Ampl.
4	Sharp	0.035	1300	0.2	0.03	0.02
	Worn	0.21	1008	0.72	0.18	0.14
5	Sharp	0.019	630	0.07	0.016	0.01
	Worn	0.15	485	0.47	0.09	0.07

Based on the new feature vectors the principal component matrixes (one for vibration and one for AE data) were computed which were next used to convert the feature space into a new set of variables, i.e. principal components being a linear combination of the original variables. These matrixes were next used to classify a verification set of features containing 24 examples for different grinding conditions.

6.1. CLASSIFICATION RESULTS

A scatter plot of the scores of the first two principal components for vibration data is shown in Fig. 12a. As may be seen, when using the first two components almost all the

grinding conditions were separated correctly. The presented results suggest that the grinding wheel wear as well as process states related to the grinding wheel thermal load and probably the workpiece thermal damage may be effectively detected using the features resulting from the HHT. In the case of AE data two distinct regions may be differentiated for the first principal component, which relates to the regions without and with the workpiece burn, see Fig. 12b. However, the scores for a sharp and worn grinding wheel may also be separated. This is due to the fact that both states, that is the wear of grinding wheel and the operation at low workpiece peripheral speeds have a similar effect on the AE signal characteristics. Summing up, the tool wear as well as the thermal damages of the grinding wheel (grain fracture) may be detected using a linear combination of only three quantities obtained from the principal component analysis.

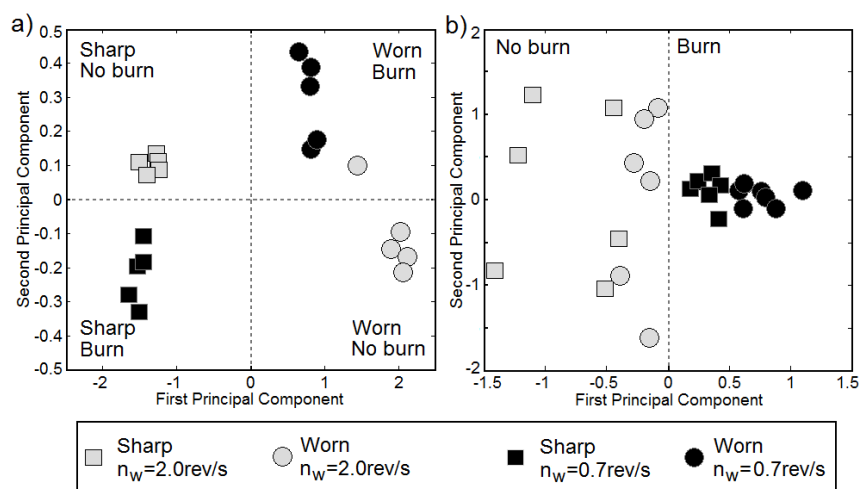


Fig. 12. Principal component scatter plot for: a) vibration and b) raw acoustic emission signal

7. CONCLUSIONS

This paper has discussed the approach of the grinding process state and tool wear diagnosis based on Hilbert-Huang transform. The analysis based on the test and real grinding data has shown that HHT transform is much better than other traditional signal processing techniques, like short-time Fourier or wavelet transform. The empirical mode decomposition method has been proved to be very effective in the separation of continuous and transient components from the vibration and raw AE signal measurements. These components can be individually studied with the use of Hilbert spectral analysis to determine instantaneous frequencies and amplitudes. Through the statistical analysis of time-dependent amplitudes and frequencies the chatter development and undesired process states related to the grinding wheel and probably the workpiece thermal damage may be effectively detected.

ACKNOWLEDGEMENT

The authors are grateful to European Regional Development Fund (Project No POIG.0101.02-00-015/08) for financial support.

REFERENCES

- [1] TÖNSHOFF H. K., FRIEMUTH T., BECKER J. C., *Process monitoring in grinding*, Annals of the CIRP 51/2/1-21.
- [2] BYRNE G., DORNFELD D., INASAKI I., KETTLER G., KÖNIG W., TETI R., 1996, *Tool condition monitoring – the status of research and industrial application*, Annals of the CIRP 44/2/541-567.
- [3] INASAKI I., KARPUSZEWSKI B., LEE H.S., 2001, *Grinding chatter – origin and suppression*, Annals of the CIRP 50/2/515-534.
- [4] WU Y., DU R., 1996, *Feature extraction and assessment using wavelet packets for monitoring of machining process*, Mechanical System and Signal Processing, 10/1/29-53.
- [5] HUANG N., et al., 1998, *The empirical mode decomposition and the Hilbert spectrum for nonlinear and nonstationary time series analysis*, Proceedings of the Royal Society, London, 903-995.
- [6] KRUSZYŃSKI B., LAJMERT P., 2005, *An intelligent supervision system for cylindrical traverse grinding*, Annals of the CIRP 54/1/305-308.
- [7] LAJMERT P., 2008, *An intelligent supervision system for optimization and control of cylindrical grinding processes*, Conf. on Selected Problems of Abrasive Machining, Bochnia, 205-214.
- [8] LAJMERT P., WRĄBEL D., 2009, *A diagnostic system for cylindrical plunge grinding process based on Hilbert-Huang transform*, Conf. on Advances of Abrasive Processes, Koszalin, 391-400.